Materials Science and Engineering B 121 (2005) 42–47

www.elsevier.com/locate/mseb

Hydrothermal preparation and optical properties of ZnO nanorods

Yong-hong Ni [a,*], Xian-wen Wei [a], Jian-ming Hong [b], Yin Ye [a]

[a] *School of Chemistry and Material Science, Anhui Normal University, Wuhu 241000, PR China*
[b] *Center of Material Analysis, Nanjing University, Nanjing 210093, PR China*

Received 9 July 2004; received in revised form 19 January 2005; accepted 26 February 2005

Abstract

In the present paper, ZnO nanorods with the mean size of 50 nm × 250 nm were successfully synthesized via a hydrothermal synthesis route in the presence of cetyltrimethylammonium bromide (CTAB). $ZnCl_2$ and KOH were used as the starting materials and zinc oxide nanorods were obtained at 120 °C for 5 h. The product was characterized by means of X-ray powder diffraction (XRD), transmission electron microscopy (TEM) and selected area electron diffraction (SAED). The optical properties of the product were studied. Some factors affecting the morphologies and optical properties were also investigated.

Keywords: Hydrothermal synthesis; Semiconductors; Nanorods; Zinc oxides

1. Introduction

Various semiconductor materials are always a research focus in material science due to their unique electronic, optical properties and extensive applications. In these materials, wide and direct band gap semiconductors are of great interest in blue and ultraviolet optical devices such as light-emitting diodes and laser diodes [1]. Zinc oxide (ZnO), as a wide and direct band gap (3.37 eV) semiconductor with a large exciton binding energy (60 meV) [2], has already been widely used in piezoelectric transducers, gas sensors, optical waveguides, transparent conductive films, varistors and solar cell windows, bulk acoustic wave devices [3–7]. With the development of material science, it is believed that ZnO has further application in many fields. Over the past decade, ZnO crystallites have been obtained by several preparation approaches including sol–gel method [8], evaporative decomposition of solution [9], wet chemical synthesis [10], gas-phase reaction [11] and hydrothermal synthesis [12], etc. A variety of morphologies including prismatic forms [13], bi-pyramidal and dumbbell-like [14], ellipsoidal [12], spheres [15], nanorods [16], nanowires [17] and whiskers [18] have been synthesized to date.

Among the above methods to prepare ZnO, hydrothermal synthesis route, as an important method for wet chemistry, has been attracting material chemists' attention. Employing this method, for instance, needle-like ZnO crystals were obtained using the decomposition of aqueous solution of Na_2Zn–EDTA at 330 °C by Nishizawa et al. [19]. Shi and coworkers prepared acicular ZnO crystals at 190 °C under the assistance of mineralized reagent of $NaNO_2$ [20]. Recently, Li's group reported the preparation of ZnO nanorods under cetyltrimethylammonium bromide (CTAB)-assisted hydrothermal route at 180 °C for 24 h using zinc powders as the initial material [21]. In this work, we designed a simple system for the preparation of ZnO nanorods employing $ZnCl_2$ and KOH as the reactants, CTAB, which is a cationic surfactant, as the directed reagent for growth of ZnO. Reactions were carried out at 120 °C for 5 h. The optical properties of the product were studied. Some factors affecting the morphologies and optical properties were also investigated.

2. Experimental

In a typical experiment, all the reagents were analytically pure and used without further purification. A 0.001 mol $ZnCl_2$

* Corresponding author. Tel.: +86 5533 883512; fax: +86 5533 869310.
E-mail address: niyh@mail.ahnu.edu.cn (Y.-h. Ni).

0921-5107/$ – see front matter © 2005 Elsevier B.V. All rights reserved.
doi:10.1016/j.mseb.2005.02.065

and 0.002 mol KOH were dissolved into small amount of distilled water, respectively, then a white floccule immediately appeared as soon as they were mixed. After 0.0005 mol CTAB was introduced under stirring, the system was transferred into a Teflon-lined stainless steel autoclave of 40 ml and filled by distilled water up to 80% volume. Hydrothermal treatments were carried out at 120 °C for 5 h. After that, the autoclave was allowed to cool down naturally. White precipitates were collected and washed with distilled water and ethanol several times to remove impurities. Finally, the precipitates were dried at 50 °C for 5 h.

This procedure was repeated using $(CH_3COO)_2Zn{\cdot}2H_2O$, $Zn(NO_3)_2{\cdot}6H_2O$ and $ZnSO_4{\cdot}7H_2O$ as the zinc source instead of $ZnCl_2$ or changing the reaction temperature.

X-ray powder diffraction (XRD) was carried out on a Rigaku (Japan) D/max-γ_A X-ray diffractometer with Cu Kα radiation ($\lambda = 0.154178$ nm) at a scanning rate of $0.02^\circ\ s^{-1}$ in the 2θ range from 10° to 70°. Transmission electron microscopy (TEM) micrographs were taken on a JEM-200CX, JEOL Transmission Electron Microscope, employing an accelerating voltage of 200 kV. UV–vis spectra were recorded on a Hitachi U-3010 spectrophotometer (Tokyo, Japan). The fluorescence spectra were measured with a F-4500 spectrofluorometer (Hitachi) with a quartz cell of 1 cm.

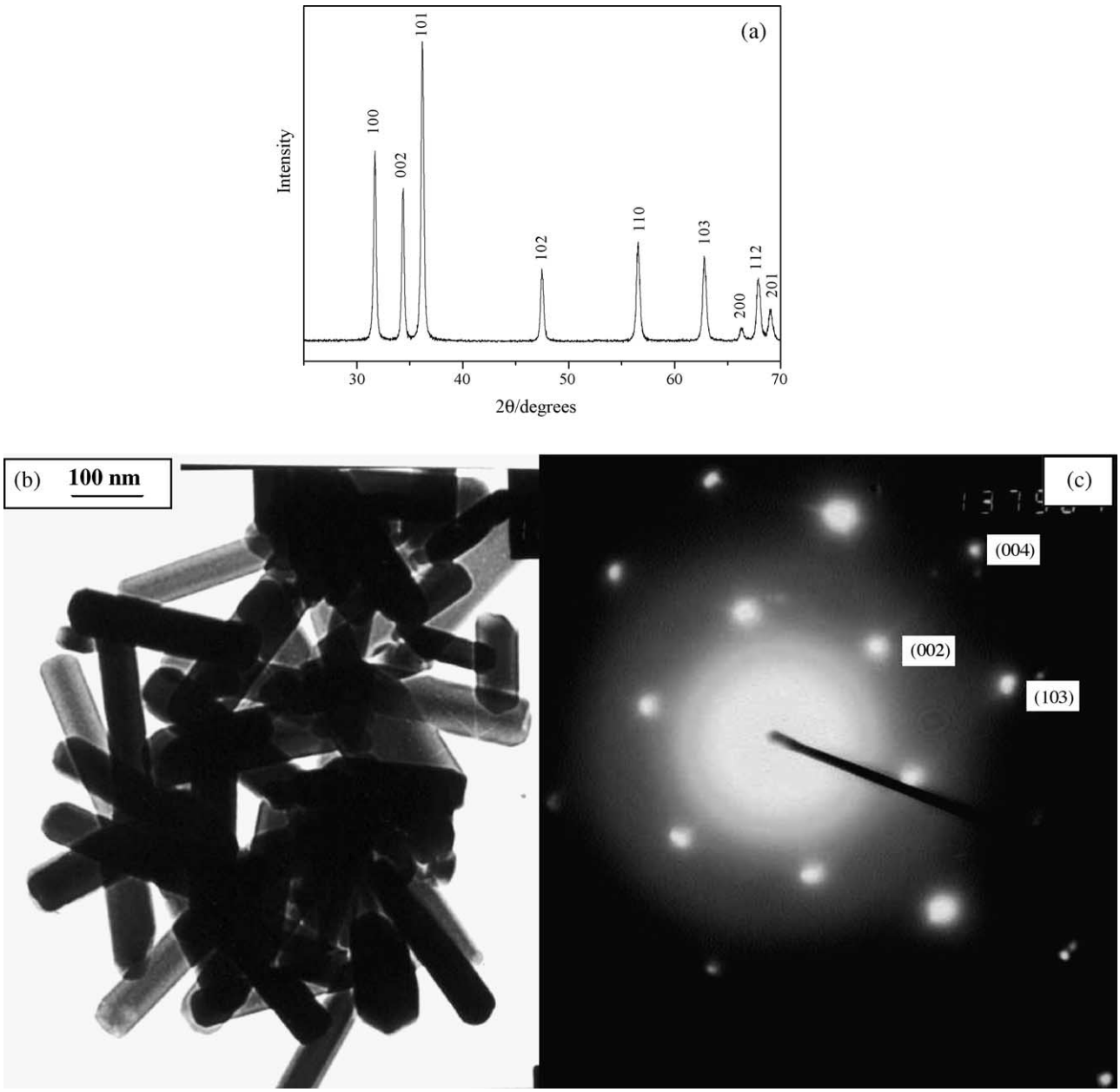

Fig. 1. (a) XRD pattern, (b) TEM image and (c) SAED pattern of ZnO nanorods prepared at 120 °C for 5 h, using $ZnCl_2$ and KOH as the reactants, CTAB as the directed reagent.

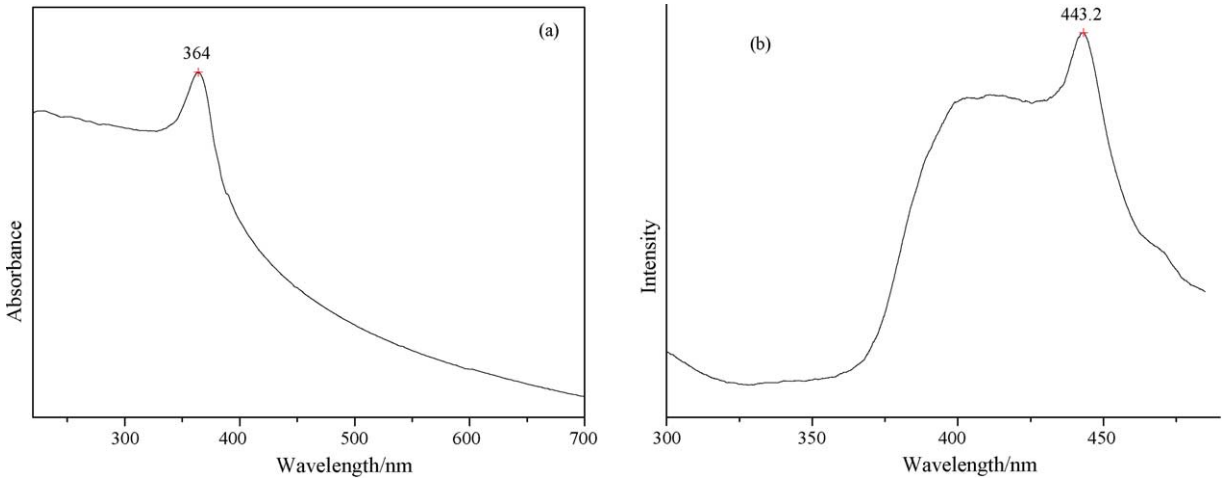

Fig. 2. (a) The absorption spectrum and (b) the emission spectrum of ZnO nanorods.

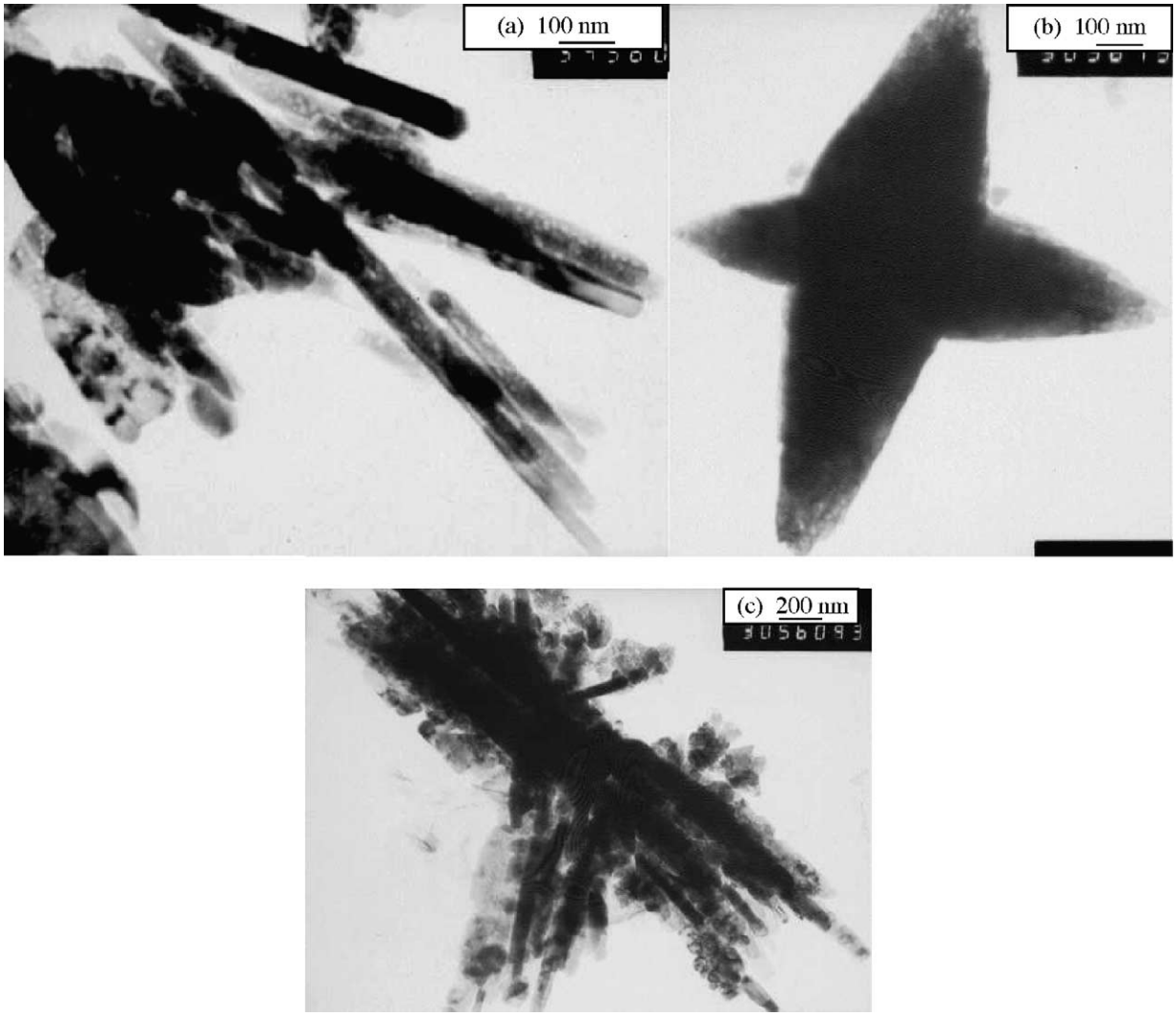

Fig. 3. TEM images of the products prepared at 120 °C for 5 h, using different zinc sources: (a) $(CH_3COO)_2Zn{\cdot}2H_2O$, (b) $Zn(NO_3)_2{\cdot}6H_2O$ and (c) $ZnSO_4{\cdot}7H_2O$.

3. Results and discussions

Fig. 1(a) shows the XRD pattern of the product. All of the diffraction peaks can be indexed within experimental error as hexagonal ZnO phase (Wurtzite-structure) with lattice constants $a = 3.2508$ Å and $c = 5.2069$ Å by comparison with the data from JCPDS cards No.36-1451. The strong and narrow diffraction peaks indicate that the material has a good crystallinity and size. No characteristic peaks from impurities such as $Zn(OH)_2$ and KCl are detected.

The TEM images of the product are given in Fig. 1(b). Many rod-like products can be clearly seen. The sizes of the products are homogeneous and the mean size is about 50 nm × 250 nm. The electron diffraction dots shown in Fig. 1(c) can be indexed as hexagonal Wurtzite-structural ZnO, which is very consistent with the analysis of XRD.

Under hydrothermal conditions, $Zn(OH)_2$ can dehydrate to produce ZnO at lower temperature (≥100 °C) [12] and generally, the growth unit for ZnO crystal is considered to be $Zn(OH)_4^{2-}$, which has a tetrahedron geometry [13]. Some ZnO crystals with a micron-scaled size have been prepared, employing $Zn(OH)_2$ as the precursor in the absence of surfactants [3,12,22]. Since a possible interaction exists in a surfactant and a precursor, it is imaginable that the morphology and size of the product are influenced by the surfactant. In our work, CTAB is a cationic surfactant and ionizes completely in water. The resulted cation is also a tetrahedron with a long hydrophobic tail [21]. Therefore, ion-pairs between $Zn(OH)_4^{2-}$ and CTA^+ could form due to electrostatic interaction [21]. In the crystallization process, surfactant molecules adsorbed on the crystal nuclei not only serve as a growth director but also as a protector to prevent from aggregation of the product. As a result, ZnO nanorods were produced.

Fig. 2(a) depicts a UV–vis spectrum of the as-prepared ZnO nanorods, which was obtained on a Hitachi U-3010 spectrophotometer by dispersing ZnO powders in distilled water and using distilled water as the reference. An absorption peak centered at 364 nm (ca. 3.41 eV) is found which has a slight blue-shift compared with that of the bulk. The PL spectrum of the as-prepared ZnO nanorods is given in Fig. 2(b), which was obtained on a F-4500 spectrofluorometer (Hitachi) with a quartz cell of 1 cm by dispersing ZnO powders in distilled water, employing the light of 250 nm as the excitation source. It is clear from the figure that the spectrum consists of a widened shoulder peak from ~400 to 430 nm and a sharp one centered at 443.2 nm. The above peak positions were very close to the recent results obtained by Gao and co-workers [23]. Usually, the UV emission is attributed to the near band edge emission of the wide band gap of ZnO due to the annihilation of excitons. And the blue luminescence is considered to be the result of radiative recombination of photo-generated holes with singularly ionized oxygen vacancies [24,25]. In our work, the stronger blue emission should be attributed to much more defective of the nanostructures prepared at lower temperature than those deposited at much higher temperatures, at which the UV emission is stronger [26].

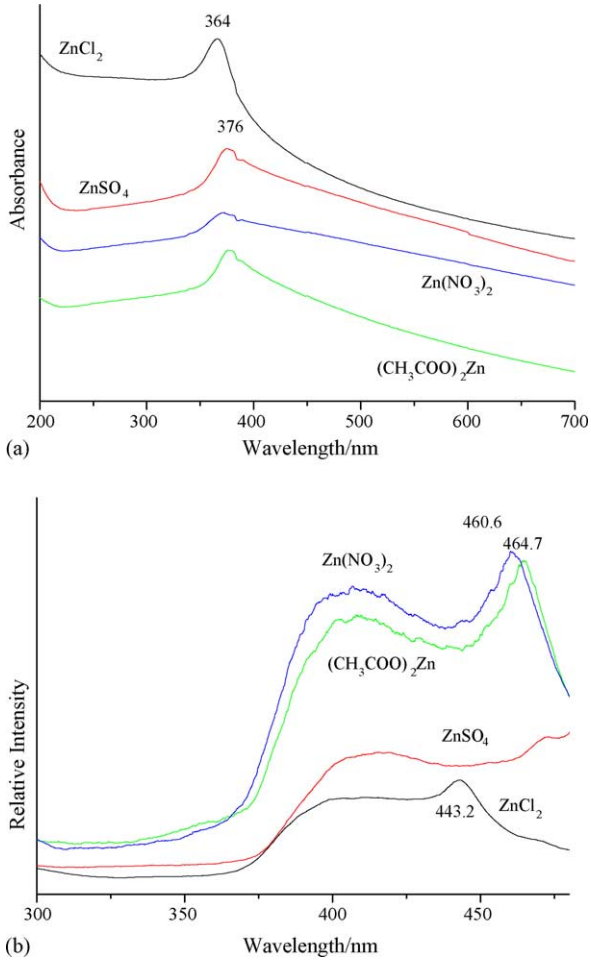

Fig. 4. (a) The absorption spectra and (b) the emission spectra of the products prepared at 120 °C for 5 h, using different zinc sources. Distilled water was used as the reference and the exciting wavelength is 250 nm.

Fig. 3 shows the TEM images of the products prepared using $(CH_3COO)_2Zn{\cdot}2H_2O$, $Zn(NO_3)_2{\cdot}6H_2O$ and $ZnSO_4{\cdot}7H_2O$ as the zinc source instead of $ZnCl_2$, respectively. As shown in TEM micrographs, some rods and flakes were obtained when $(CH_3COO)_2Zn{\cdot}2H_2O$ and $ZnSO_4{\cdot}7H_2O$ were used as the zinc source, while $Zn(NO_3)_2{\cdot}6H_2O$ as the zinc source, some elliptic products were produced. The absorption spectra in Fig. 4(a) shows that the products have a similar absorption peak located at 376 nm when $(CH_3COO)_2Zn{\cdot}2H_2O$, $Zn(NO_3)_2{\cdot}6H_2O$ and $ZnSO_4{\cdot}7H_2O$ were employed as the zinc source instead of $ZnCl_2$. Compared with that of ZnO nanorods prepared using $ZnCl_2$ as the zinc source, the absorption peak red-shifts 12 nm. Fig. 4(b) is PL spectra of the products prepared using the different zinc sources. All the emission spectra range from 375 to 475 nm, indicating that the PL spectra were not influenced by the change of the zinc source. The broad peaks centered at ca. 405 nm are attributed to the recombination of free excitons and the peaks behind 460 nm should come from oxygen vacancy of the products.

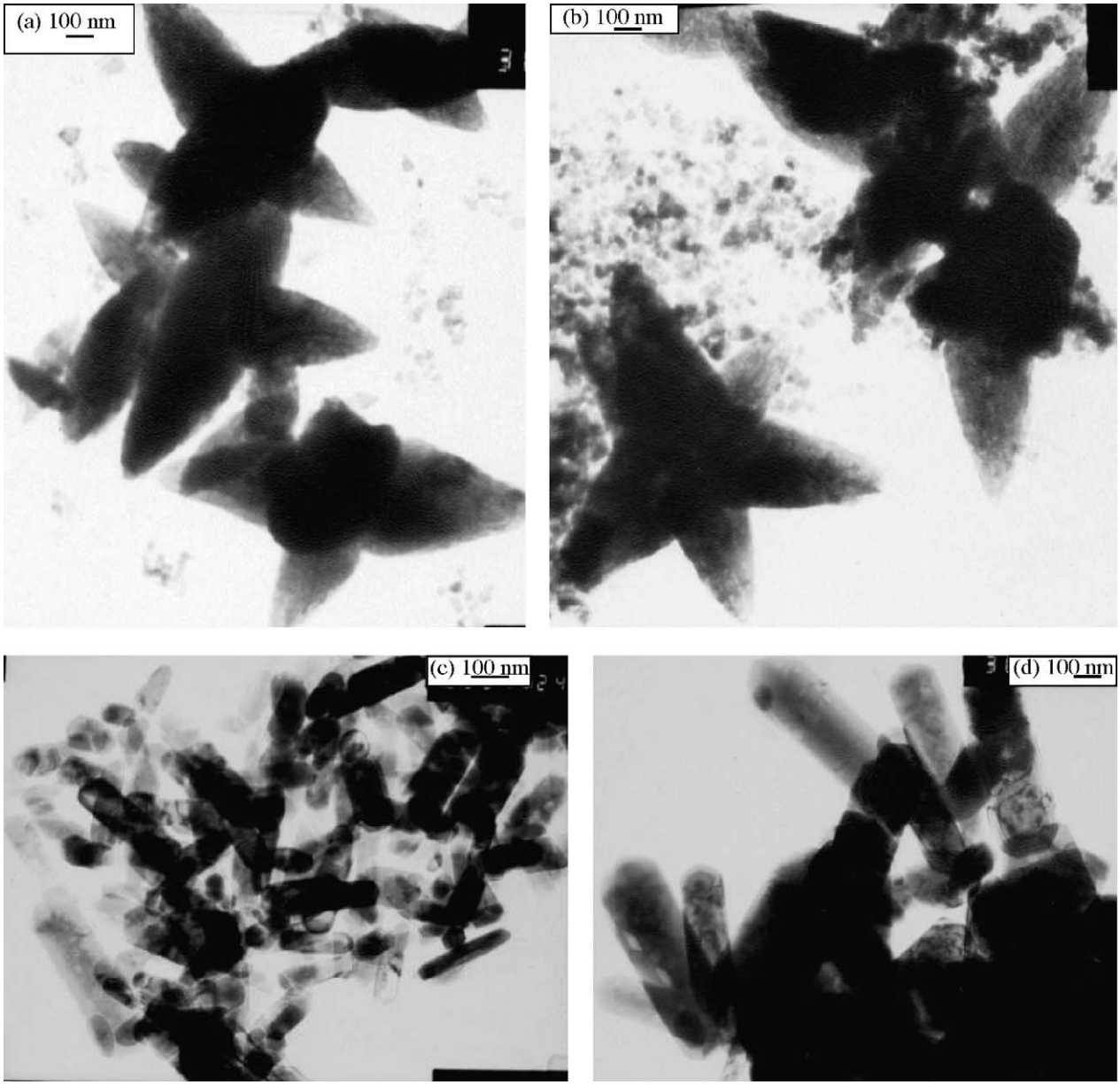

Fig. 5. TEM images of the products prepared at various temperatures for 5 h: (a) 100 °C, (b) 150 °C, (c) 180 °C and (d) 200 °C.

Fig. 5 depicts the TEM images of the products synthesized at various reaction temperatures for the same time. When the temperatures of 100 and 150 °C were employed, the main shape of the products is elliptic, while when the temperatures are 180 and 200 °C, the main shape of the products is rod-like. The absorption spectra of the products synthesized at various reaction temperatures show that the absorption peak gradually shifts from 360, 366, 376 to 377 nm with the increase of the reaction temperature from 100 to 200 °C (Fig. 6(a)). The PL spectra given in Fig. 6(b) shows that all the products have a similar emission spectrum, which comprised a strong emission peak centered at ca. 404 nm and a weak UV emission peak at 353 nm. In 2003, Agostiano and co-workers also found the weak UV emission peak [27]. Generally, the dominance of the UV emission at 353 nm in PL spectra has been rarely observed for ZnO nanocrystals, except when their surface has been passivated by organic molecules or when the particles from alcoholic solutions have been UV-irradiated in airless conditions [27]. In our work, it is probable that ZnO surface in our samples was partially passivated by CTAB. As a result, the UV luminescence can be responsibly detected.

From the above experiments, one can easily find that the morphologies and absorption properties of the products can be influenced when zinc source or reaction temperature varied, while the PL spectra not change generally.

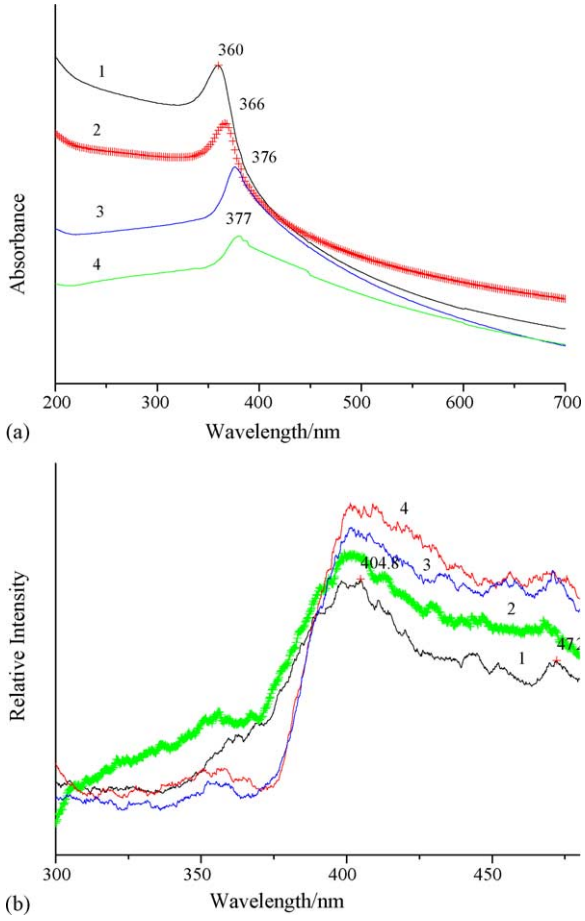

Fig. 6. (a) The absorption spectra and (b) the emission spectra of the products prepared at various reaction temperatures for 5 h: (1) 100 °C, (2) 150 °C, (3) 180 °C and (4) 200 °C. Distilled water was used as the reference and the exciting wavelength is 250 nm.

4. Conclusions

ZnO nanorods have been successfully synthesized in a simple system at 120 °C for 5 h via the hydrothermal method. $ZnCl_2$ and KOH were used as the reactants and CTAB as the directed reagent for growth of ZnO. The absorption peak of the as-obtained ZnO nanorods has a slight blue-shift compared with that of the bulk. Experiments showed that the different zinc source and reaction temperature would influence morphologies and absorption properties of the final products but the PL spectra not change generally.

Acknowledgement

We thank Anhui Provincial Excellent Young Scholars Foundation (No. 04046065) for fund support.

References

[1] B.J. Jin, S.H. Bae, S.Y. Lee, S. Im, Mater. Sci. Eng. B 71 (2000) 301.
[2] P. Zu, Z.K. Tang, G.K.L. Wong, M. Kawasaki, A. Ohtomo, H. Koinuma, Y. Segawa, Solid State Commun. 103 (1997) 459.
[3] E. Ohshima, H. Ogino, I. Niikura, K. Maeda, M. Sato, M. Ito, T. Fukuda, J. Cryst. Growth 260 (2004) 166.
[4] T.L. Yang, D.H. Zhang, J. Ma, H.L. Ma, Y. Chen, Thin Solid Films 326 (1998) 60.
[5] B. Sang, A. Yamada, M. Konagai, Jpn. J. Appl. Phys. 37 (1998) L206.
[6] J.F. Cordaro, Y. Shim, J.E. May, J. Appl. Phys. 60 (1986) 4186.
[7] P. Verardi, N. Nastase, C. Gherasim, C. Ghica, M. Dinescu, R. Dinu, C. Flueraru, J. Cryst. Growth 197 (1999) 523.
[8] R.J. Lanf, W.D. Bond, Am. Ceram. Soc. Bull. 63 (1984) 278.
[9] E. Ivers-Tiffee, K. Seitz, Am. Ceram. Soc. Bull. 66 (1987) 1384.
[10] N.Y. Lee, M.S. Kim, J. Mater. Sci. 26 (1991) 1126.
[11] S.M. Haile, D.W. Jonhagon, G.H. Wiserm, J. Am. Ceram. Soc. 72 (1989) 2004.
[12] C.H. Lu, C.H. Yeh, Ceram. Int. 26 (2000) 351.
[13] W.J. Li, E.W. Shi, W.Z. Zhong, Z. Yin, J. Cryst. Growth 203 (1999) 186.
[14] B.G. Wang, E.W. Shi, W.Z. Zhong, Cryst. Res. Technol. 33 (1998) 937.
[15] M.C. Neves, T. Trindade, A.M.B. Timmons, J.D. Pedrosa de Jesus, Mater. Res. Bull. 36 (2001) 1099.
[16] J. Zhang, L. Sun, H. Pan, C. Liao, C. Yan, New J. Chem. 26 (2002) 33.
[17] C. Xu, G. Xu, Y. Liu, G. Wang, Solid State Commun. 122 (2002) 175.
[18] J.Q. Hu, Q. Li, N.B. Wong, C.S. Lee, S.T. Lee, Chem. Mater. 14 (2002) 1216.
[19] H. Nishizawa, T. Tani, K. Matsuka, J. Am. Ceram. Soc. 67 (1984) C-98.
[20] W.J. Li, E.W. Shi, J. Mater. Res. 14 (1999) 1532.
[21] X.M. Sun, X. Chen, Z.X. Deng, Y.D. Li, Mater. Chem. Phys. 78 (2002) 99.
[22] H. Xu, H. Wang, Y. Zhang, S. Wang, M. Zhu, H. Yan, Cryst. Res. Technol. 38 (2003) 429.
[23] J.M. Wang, L. Gao, J. Cryst. Growth 262 (2004) 290.
[24] C.L. Xu, D.H. Qin, H. Li, Y. Guo, T. Xu, H.L. Li, Mater. Lett. 58 (2004) 3976.
[25] K. Vanheusden, W.L. Warren, C.H. Seager, D.R. Tallant, J.A. Voigt, B.E. Gnade, J. Appl. Phys. 79 (1996) 7983.
[26] Y. Sun, G.M. Fuge, M.N.R. Ashfold, Chem. Phys. Lett. 396 (2004) 21.
[27] P.D. Cozzoli, M.L. Curri, A. Agostiano, G. Leo, M. Lomascolo, J. Phys. Chem. B 107 (2003) 4756.